Profound Steric Control of Reactivity in Aryl Halide Addition to Bisphosphane Palladium(0) Complexes**

Erwan Galardon, Shailesh Ramdeehul, John M. Brown,* Andrew Cowley, King Kuok (Mimi) Hii, and Anny Jutand

The application of bulky electron-rich phosphanes typified by P*t*Bu$_3$ has permitted significant new advances in palladium-catalyzed cross-couplings and aminations.[1] Recent work by Roy and Hartwig indicates that the enhanced reactivity may be associated with a change in mechanism of the oxidative-addition step compared to, for example, PPh$_3$ complexes; the intervention of monoligated [PdP*t*Bu$_3$] species is strongly implicated by studies of the reverse ArX elimination, observed indirectly.[2] Notably, the successful palladium-catalyzed coupling of alkyl boranes with alkyl halides without competing β-elimination requires the less bulky PCx$_3$ (Cx = cyclohexyl), and P*t*Bu$_3$ is ineffective.[3]

We report here that the mechanism of the ArX addition step to zerovalent [PdL$_2$] complexes is highly sensitive to the bulk of the ligand L, by study of the series of complexes [Pd(PCx$_n$*t*Bu$_{3-n}$)$_2$]; $n = 0-3$. The ligands PCx$_2$*t*Bu **1** and PCx*t*Bu$_2$ **2** were prepared from known compounds Cx$_2$PCl and CxPCl$_2$, by reaction with *t*BuLi at $-78\,^{\circ}$C,[4] and converted into the corresponding complexes [Pd(PCx$_2$*t*Bu)$_2$] (**3**) and [Pd(PCx*t*Bu$_2$)$_2$] (**4**), by reaction with [C$_5$H$_5$PdC$_3$H$_5$].[5] Complexes [Pd(PCx$_3$)$_2$] (**5**) and [Pd(P*t*Bu$_3$)$_2$] (**6**) have already been described; both are commercially available. Attempted Heck reaction between *n*-butyl acrylate and chlorobenzene as previously described,[6] indicated the clear distinction between complexes **3** or **5** which were ineffective, and **4** or **6** which were comparably effective (Scheme 1). This points to crucial differences between the ligands with one and two *tert*-butyl groups.

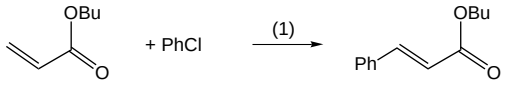

Ligand	PCx$_3$	**1**	**2**	P*t*Bu$_3$
Yield [%]	0	7	53	58

Scheme 1. 1) 1.5 mol% [Pd$_2$(dba)$_3$], 6% ligand, Cs$_2$CO$_3$ (1.1 equiv), 120 °C, 40 h; C$_{13}$H$_{28}$ as GC internal standard. dba = *trans*,*trans*-dibenzylideneacetone

The addition of PhI to complex **5** in THF occurs very rapidly; tenfold excess of added ligand did not cause any evident inhibition and the sole product is the *trans* bisphosphane complex **7**. The reaction with PhOTf (Tf = triflate), which is slower by a factor of about sixty, was studied in detail by electrochemical techniques at 25 °C. Under these conditions, the reaction follows an associative mechanism, as the rate is unaffected by the addition of excess PCx$_3$, within experimental error (Figure 1a). These observations contrast with the known mechanism of ArBr addition to [Pd(P(*o*-tolyl)$_3$)$_2$],[7] where dissociation of one phosphane ligand precedes addition of the electrophile and the product is the halide-bridged dimer **8**.[8]

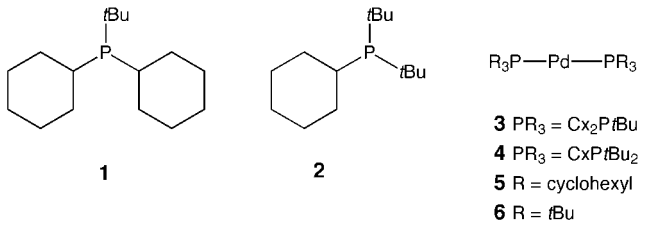

1 **2**

3 PR$_3$ = Cx$_2$P*t*Bu
4 PR$_3$ = CxP*t*Bu$_2$
5 R = cyclohexyl
6 R = *t*Bu

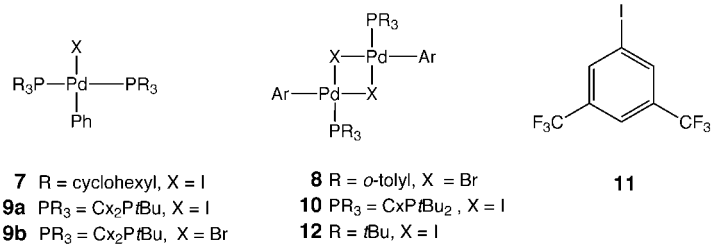

7 R = cyclohexyl, X = I
9a PR$_3$ = Cx$_2$P*t*Bu, X = I
9b PR$_3$ = Cx$_2$P*t*Bu, X = Br

8 R = *o*-tolyl, X = Br
10 PR$_3$ = CxP*t*Bu$_2$, X = I
12 R = *t*Bu, X = I

11

The more slowly reacting complex **3** proved to be too air-sensitive for electrochemical studies under these conditions. By monitoring its reaction with PhI by ^{1}H NMR spectroscopy, we established that an associative mechanism was again followed, albeit around 10^3 times slower than in the case of complex **5**, and again without inhibition by excess ligand (Figure 1b). The ^{1}H NMR spectrum of the product **9a** showed the characteristic virtual coupling in the *t*Bu resonance signal, associated with *trans*-L$_2$M geometry (M = metal center).[9] When the initial reaction was carried out with PhBr, the product **9b** could be isolated and characterized by X-ray crystallography, which demonstrates the lack of steric distortion of the coordination sphere, although some van der Waals strain is apparent. The Ph group is sandwiched between opposing cyclohexyl rings (Figure 2).[10]

[*] Dr. J. M. Brown, Dr. E. Galardon, Dr. S. Ramdeehul
Dyson Perrins Laboratory
South Parks Road, Oxford, OX1 3QY (UK)
Fax: (+44) 1865-275642
E-mail: bjm@herald.ox.ac.uk.
Dr. A. Cowley
Chemical Crystallography Laboratory
Parks Road, Oxford, OX1 3QZ (UK)
Dr. K. K. (Mimi) Hii
Department of Chemistry, King's College
Strand, London, WC2R 2LS (UK)
Dr. A. Jutand
Ecole Normale Superieure, Departement de Chimie
CNRS UMR 8640, 24 Rue Lhomond 75231 Paris Cedex 5 (France)

[**] We thank the EPSRC for support (PDRA posts for E.G. and S.R., purchase of diffractometer) and Johnson-Matthey for the loan of Pd salts. Dr. R. T. Aplin was very helpful in the acquisition of electrospray MS.

Supporting information for this article is available on the WWW under http://www.angewandte.com or from the author.

  1433-7851/02/4110-1760 $ 20.00+.50/0

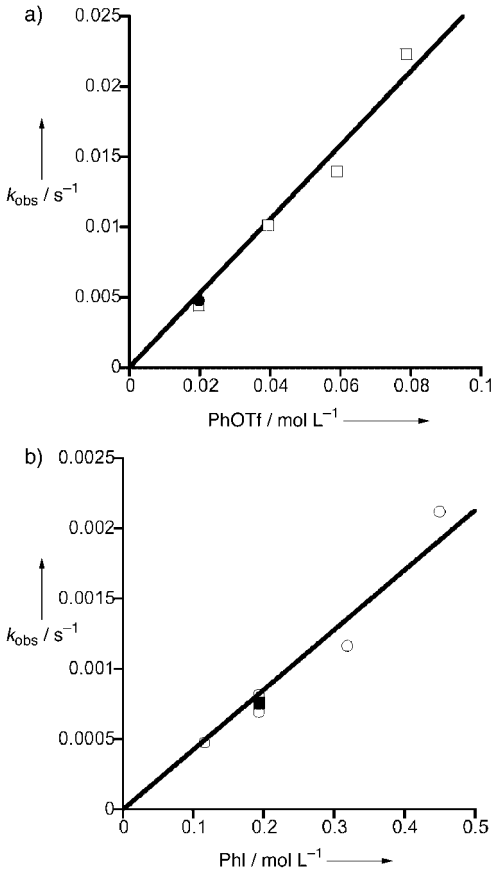

Figure 1. a) Reaction of PhOTf with complex **5**, monitored by amperometry in THF at 25 °C; k_{obs}/[PhOTf] = 0.26 $M^{-1} s^{-1}$; b) Reaction of PhI with complex **3** at 22 °C monitored by ^1H NMR spectroscopy in C_6D_6; k_{obs}/[PhI] = 0.0045 $M^{-1} s^{-1}$. Runs with □ or ○ were carried out with equimolar complex and electrophile, ● in (a) with 30-fold excess PCx_3; ■ in (b) with tenfold excess PCx_2tBu. In (a), the reaction with PhI is about sixty times faster and is unaffected by excess PCx_3.

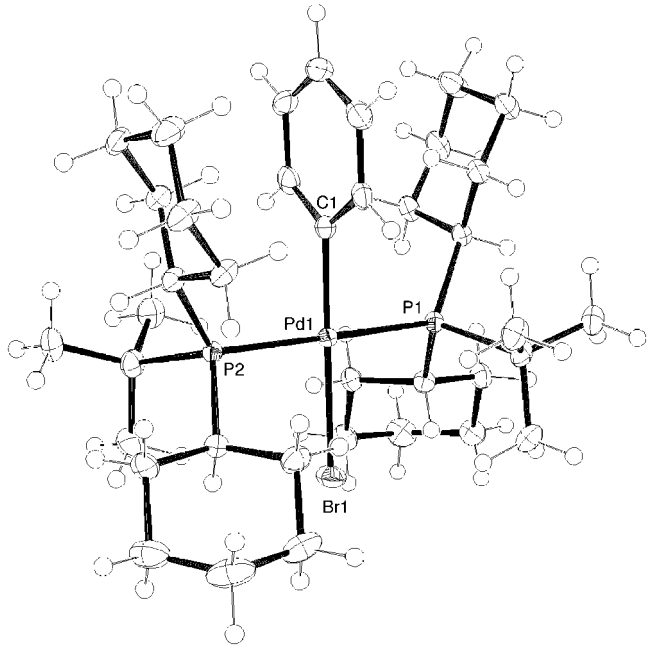

Figure 2. Molecular structure of **9b**. Selected bond lengths [Å] and angles [°]: Pd1-P1 2.3963(7), Pd1-P2 2.4020(7), Pd1-Br1 2.5596(3), Pd1-C1 1.997(3); Br1-Pd1-P1 89.624(18), P1-Pd1-P2 178.81(2), Br1-Pd1-C1 178.93(8), P1-Pd1-C1 90.66(7), P2-Pd1-C1 88.99(7).

Treatment of **4** with PhBr lead to the slow generation of a monophosphane palladium complex and an equivalent of free phosphane. With the more strongly electrophilic halide **11**, it was shown that doubling the concentration of excess phosphane inhibited the rate by a factor of two, in C_6D_6 at 22 °C. This places the reaction in the same mechanistic class as that of [Pd(P(*o*-tolyl)$_3$)$_2$], described above, with reversible phosphane dissociation preceding the addition of electrophile to a monoligated species [PdL]. The ^{31}P NMR spectrum of product **10**, from the addition of PhI, indicates complex temperature-dependent equilibria. In parallel experiments, very slow addition of PhI to the tBu_3P-derived complex **6** was detected and, after 4 days at RT, the solution contained one equivalent of free phosphane and one equivalent of dimer **12**, characterized by NMR spectroscopy. On redissolution, **12** was readily converted into biphenyl and the known Pd–Pd dimer **13**.[11] This behavior was not observed for the related complex **10** described above.

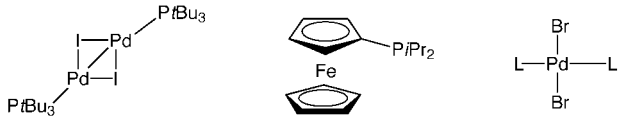

13 **14** **15** L = **14**

The presence of distinct reaction pathways of oxidative addition for the two closely related complexes **3** and **4** indicates an extreme sensitivity to steric environment, as does the gross difference in reactivity between **3** and **5**, which react by the same mechanism. This was elaborated by semiempirical calculations of the optimum energy and geometry for the sequence of [Pd(X)L_2Ph] complexes (X = Cl, Br, I), and their [PdL_2] precursors; the [Pd(I)L_2Ph] complexes are shown in Figure 3.[12] The evident increase in steric crowding demonstrates that *sec*-alkyl substituents on phosphorus ligands permit the formation of the square-planar *trans* bisphosphane-addition complexes more easily, with a substantial enthalpy penalty arising from each additional *tert*-alkyl group.

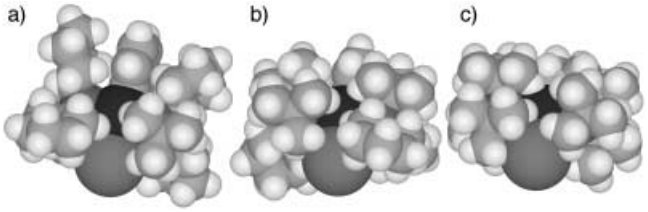

Figure 3. PM3-derived space-filling models of complexes a) [Pd(I)-(Cx_2tBuP)$_2$Ph] (**9a**); b) [Pd(I)($CxtBu_2P$)$_2$Ph]; c) [Pd(I)(tBu_3P)$_2$Ph], which demonstrates the progressive increase in crowding in the region of the Ph and I units.

The results summarized in Scheme 2 support the general conclusion that the less bulky ligands **1** and PCx_3 initiate coupling reactions through the initial formation of *trans*-[Pd(X)L_2R], whilst the bulkier ligands **2** and $PtBu_3$ generate

  1433-7851/02/4110-1761 $ 20.00+.50/0

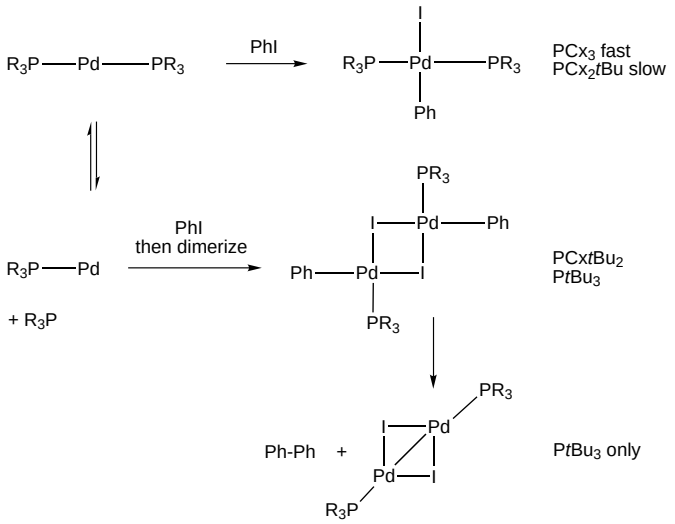

Scheme 2. Summary of the reactivities and reaction pathways for the oxidative additions of PhI to the Pd^0 complexes described.

[{Pd(X)LR}$_2$] species from a monoligated reactant. Easy access to the former structure can sometimes provide significant disadvantages for coupling chemistry. For example, the electron-rich but less bulky ligand **14** is effective in the reaction outlined in Scheme 3, but only for about 40 turnovers with about 15% of both biaryl and C–Br reduction product formed in side-reactions.[13] The loss of activity correlates well with the observed formation of the X-ray characterized complex **15**,[10] which quite rapidly becomes the sole Pd-containing species in the reaction when followed by NMR spectroscopy. It was separately confirmed that complex **15** is noncatalytic in this procedure.

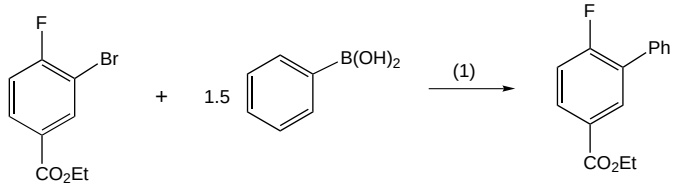

Scheme 3. 1) 1 mol% $Pd(OAc)_2$, 2 mol% ligand **14**, Cs_2CO_3 (2 equiv), toluene, RT.

In conclusion, the effectiveness of P*t*Bu$_3$ and ligand **4** in Pd couplings of unsaturated electrophiles is associated with a propensity to form monophosphane complexes, either as, or en route to, the true catalytic species. Steric inhibition of the formation of [Pd(X)L$_2$Ar] and [Pd(X)$_2$L$_2$] *trans* diphosphane complexes must play an important role here. In alkyl–alkyl couplings,[3] the accessibility of stable *trans*-[L$_2$Pd(X)R] and *trans*-[L$_2$PdRR′] complexes is likely to be important in directing the reaction from β-elimination towards C–C bond formation after the initial RX addition step. Hence, it is to be expected that different palladium-catalyzed reactions will respond to different ligation states, but in a potentially predictable way.

Experimental Section

NMR studies: Kinetic experiments were performed at 22 °C with 0.013 M solutions of palladium complex in C_6D_6 for **3** and 0.015 M for **4**. After addition of the aryl iodide, spectra were then recorded at regular time intervals until the conversion reached about 50%. The data were acquired by following the disappearance of one of the cyclohexyl signals (δ = 2.44 ppm for **3**, δ = 2.70 ppm for **4**) and/or the *t*Bu signal (δ = 1.51 ppm for **3** and δ = 1.48 ppm for **4**).

Electrochemical studies: Kinetic experiments were performed at 25 °C with 0.0016 M solutions of [Pd(PCx$_3$)$_2$] in THF. The data were acquired by following the disappearance of the oxidation current of [Pd(PCy$_3$)$_2$] at a rotating gold disk electrode polarized at +0.3 V versus saturated calomel electrode (SCE). The electrochemical procedure has been described.[14]

Oxidative addition products:

9a: ^{1}H NMR (250 MHz, C_6D_6): δ = 1.25–2.09 (m, 44H, Cx), 1.69 (t, 18H, ^3J + ^5J = 12.4 Hz, *t*Bu), 6.93–7.05 (m, 3H, Ar), 7.69 ppm (m, 2H, Ar); ^{31}P NMR (101 MHz, C_6D_6): δ = 32.6 ppm (br).

10: ^{1}H NMR (250 MHz, C_6D_6): δ = 0.97–1.92 (m, 11H, Cx), 1.45 (d, 18H, 12.6 Hz, *t*Bu), 6.90 (t, 1H, 7.2 Hz, Ar), 7.07 (t, 2H, 7.8 Hz, Ar), 7.86 ppm (d, 2H, 7.8 Hz, Ar); ^{31}P NMR (101 MHz, C_6D_6): δ = 64.4 ppm (s).

12: ^{1}H NMR (250 MHz, C_6D_6): δ = 1.09 (d, 27H, 12.5 Hz, *t*Bu), 6.87 (m, 3H, Ph), 7.47 ppm (m, 2H, Ph); ^{31}P NMR (101 MHz, C_6D_6) δ = 57.9 ppm (s).

Synthetic procedures are recorded in the Supporting Information.[15]

Received: November 12, 2001 [Z18197]

[1] A. F. Littke, G. C. Fu, *J. Org. Chem.* **1999**, *64*, 10–12; A. F. Littke, C. Dai, G. C. Fu, *J. Am. Chem. Soc.* **2000**, *122*, 4020–4028; S. Lee, M. Jorgensen, J. F. Hartwig, *Org. Lett.* **2001**, *3*, 2729–2732; C. Dai, G. C. Fu, *J. Am. Chem. Soc.* **2001**, *123*, 2719–2724; S. Lee, M. Jorgensen, J. F. Hartwig, *Org. Lett.* **2001**, *3*, 2729–2732; for the original work on this ligand see: T. Yoshida, S. Otsuka, *Inorg. Synth.* **1990**, *28*, 113–119; T. Yoshida, S. Otsuka, *J. Am. Chem. Soc.* **1977**, *99*, 2134–2140; S. Otsuka, T. Yoshida, M. Matsumoto, K. Nakatsu, *J. Am. Chem. Soc.* **1976**, *98*, 5850–5858.

[2] A. H. Roy, J. F. Hartwig, *J. Am. Chem. Soc.* **2001**, *123*, 1232–1233.

[3] M. R. Netherton, C. Dai, K. Neuschütz, G. C. Fu, *J. Am. Chem. Soc.* **2001**, *123*, 10099–10100.

[4] For example, E. Niecke, M. Leuer, M. Nieger, *Chem. Ber.* **1989**, *122*, 453–461; for a recent preparation of compound **3** see: D. Jan, L. Delaude, F. Simal, A. Demonceau, A. F. Noels, *J. Organomet. Chem.* **2000**, *606*, 55–64.

[5] T. Yoshida, S. Otsuka, *Inorg. Synth.* **1985**, *28*, 113–119.

[6] F. Ozawa, N. Kawasaki, H. Okamoto, T. Yamamoto, A. Yamamoto, *Organometallics* **1987**, *6*, 1640–1651.

[7] F. Paul, J. Patt, J. F. Hartwig, *Organometallics* **1995**, *14*, 3030–3039; J. F. Hartwig, F. Paul, *J. Am. Chem. Soc.* **1995**, *117*, 5373–5374.

[8] For related X-ray structures see: A. L. Rheingold, W. C. Fultz, *Organometallics* **1984**, *3*, 1414–1417; V. V. Grushin, H. Alper, *Organometallics*, **1993**, *12*, 1890–1901.

[9] G. M. Whitesides, J. F. Gaasch, *J. Organomet. Chem.* **1971**, *33*, 241–246; J. P. Fackler, Jr., J. A. Fetchin, J. Mayhew, W. C. Seidel, T. J. Swift, M. Weeks, *J. Am. Chem. Soc.* **1969**, *91*, 1941–1947, and references therein.

[10] Crystal structure data for **9b**: $C_{38}H_{67}BrP_2Pd$, M_r = 772.20, monoclinic, space group $P2_1/c$, a = 12.4106(1), b = 10.0836(1), c = 30.0611(3) Å, α = 90, β = 91.1483(4), γ = 90°, cell volume = 3761.2 Å^3, Z = 4, R = 0.0297. The crystal structure of **15** is given in the Supporting Information and the full details of crystal structures are deposited with the Cambridge Crystallographic Data Centre. CCDC-173949 (**9b**) and CCDC-173948 (**15**) contain the supplementary crystallographic data for this paper. These data can be obtained free of charge via www.ccdc.cam.ac.uk/conts/retrieving.html (or from the Cambridge Crystallographic Data Centre, 12, Union Road, Cambridge CB2 1EZ, UK; fax: (+44) 1223-336-033; or deposit@ccdc.cam.ac.uk).

  1433-7851/02/4110-1762 $ 20.00+.50/0

[11] V. Dura-Vila, M. P. D. Mingos, R. Vilar, A. J. P. White, D. J. Williams, *J. Organomet. Chem.* **2000**, *600*, 198–205, and references therein.
[12] Calculations at the PM3 level (MacSpartan Pro) on the complete series of complexes [Pd(X){tBu$_n$$iPr_{3-n}$)P}$_2$Ph]; X = Cl, Br, I and the [PdL$_2$] parents, reveal that a progressive increase in strain occurs in both the linear complexes and their PhX addition products with increasing tBu substitution. For the reaction in Equation (1), ΔH_r is 0, 7.8, 15.6, and 39.8 Kcal mol^{-1} for PiPr$_3$ (standard), P(iPr)$_2$$tBu, Pi$Pr($t$Bu)$_2$, and P$tBu_3$. These trends were confirmed when ligands **1** and **2** were employed in the calculations.

$$[PdL_2] + PhI \rightarrow [Pd(I)L_2(Ph)] + \Delta H_r \quad (1)$$

[13] W. R. Cullen, S. J. Rettig, T. C. Zheng *Organometallics* **1992**, *11*, 3434–3439.
[14] A. Jutand, K. K. Hii, M. Thornton-Pett, J. M. Brown, *Organometallics* **1999**, *18*, 5367–5374.
[15] Experimental details are recorded in the Supporting Information.

Weak Distance Dependence of Excess Electron Transfer in DNA**

Christoph Behrens, Lars T. Burgdorf, Anja Schwögler, and Thomas Carell*

Electron transfer phenomena in DNA are of fundamental importance for DNA damage[1] and DNA repair.[2] In this context, the movement of a positive charge (hole) through DNA has been studied intensively over the past few years.[3–6] After a controversial debate about the "hole conductivity" of double-stranded DNA,[7, 8] it is now accepted that a positive charge can move through DNA over significant distances.[9] Two mechanisms, namely coherent superexchange for small transfer distances[10, 11] and hole[4] or polaron hopping[6] for long-range transfer are evoked to describe this phenomenon. Experimentally, it is becoming clear that long-range hole transfer requires intermediate guanines and to a lesser extent also adenines to function as temporarily oxidizable "stepping stones".[12] Whether long-range hole transfer has biological consequences is unclear, but there are speculations that the process might define the genome sites damaged during oxidative stress.[13]

In contrast to hole transfer, little is known about the transport of excess electrons (negative charges) through a DNA duplex.[14, 15] Such an excess electron transfer, however, is important in biology because DNA photolyase enzymes[16–18] repair UV-induced cyclobutane pyrimidine dimer lesions in the DNA duplex by an electron transfer from a reduced and deprotonated FADH$^-$ cofactor to the dimer lesion.[19] The cytotoxic and mutagenic dimer lesions undergo rapid cycloreversion after one-electron reduction, which rescues cells from UV-induced cell death.[20] Recently γ-radiolysis together with electron paramagnetic resonance (EPR) studies provided initial evidence that excess electrons might also move through the DNA duplex by thermally activated hopping.[21–24] In the reductive regime, however, thymines and cytosines are predicted to function as "stepping stones" because they are the most easily reduced nucleobases.[25, 26]

We report here on the distance dependence of an excess electron transfer in a defined donor–DNA–acceptor system recently introduced by us as a photolyase mimic.[27, 28] In DNA double strands like **1** (Scheme 1), the electron flows from a photoexcited reduced flavin electron donor to a thymine dimer acceptor, separated by adenine:thymine bridges (A:T)$_n$ of various lengths. The electron injection is initiated by irradiation of the DNA double strand at 360 nm which causes excitation of the reduced and deprotonated flavin donor. The injected electron can either recombine with the resulting neutral flavin radical or it can move until it reduces the thymine dimer **1**→**2**. The negative charge captured by the dimer subsequently triggers a cycloreversion **2**→**3**. To allow rapid quantification of this dimer reversal step, we introduced a special dimer into the DNA strand, which lacks the connecting phosphodiester unit between the 3′- and 5′-

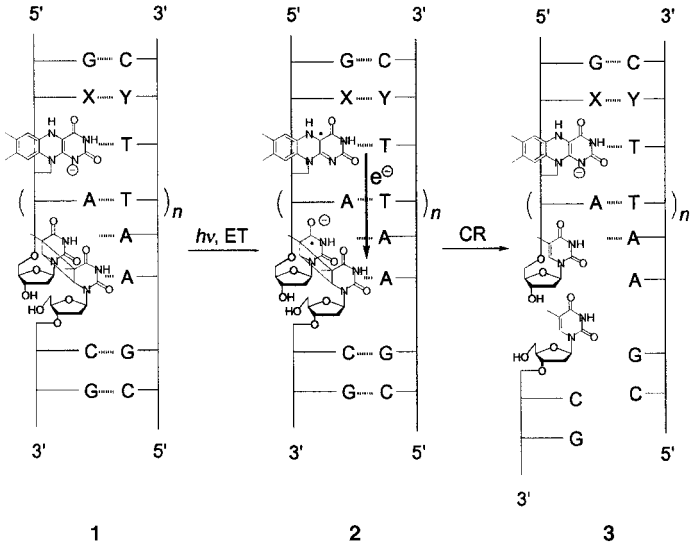

Scheme 1. Depiction of the DNA double strands containing the reduced flavin electron injector and the dimer electron acceptor. Photoexcitation ($h\nu$) initiates charge injection and transfer of the negative charge (ET) to the dimer unit (**1**→**2**). This causes cycloreversion (CR) of the dimer, which is accompanied by a strand break (**2**→**3**). Photolysis was performed in a fluorimeter (JASCO) equipped with a 150-W xenon lamp and a monochromator (10-nm band path) at 360 nm and at pH 9 (Tris buffer). Irradiations were carried out after reduction of the flavin in the DNA duplex by addition of sodium dithionite solution in the absence of oxygen at 10 °C.

[*] Prof. Dr. T. Carell, Dipl.-Chem. C. Behrens, Dipl.-Chem. L. T. Burgdorf, Dr. A. Schwögler
Fachbereich Chemie
Philipps-Universität Marburg
Hans-Meerwein-Straße, 35032 Marburg (Germany)
Fax: (+49) 6421-282-2189
E-mail: carell@mailer.uni-marburg.de

[**] We thank B. Giese, F. Hensel, and M. E. Michel-Beyerle for intensive discussions and two referees for providing valuable insights into the photochemistry of the reaction. This work was supported by the Volkswagenstiftung, the Fonds der Chemischen Industrie, and the Boehringer Ingelheim Fonds (predoctoral fellowship to L.T.B.).

  1433-7851/02/4110-1763 $ 20.00+.50/0